

1 **Slow neural oscillations explain temporal fluctuations in distractibility**

2

3 Troy Ka-Yan Lui^{1,2}, Jonas Obleser^{1,2}, & Malte Wöstmann^{1,2}

4 1. Department of Psychology, University of Lübeck, Ratzeburger Allee 160, 23562
5 Lübeck, Germany

6 2. Center of Brain, Behavior and Metabolism, University of Lübeck, Ratzeburger Allee
7 160, 23562 Lübeck, Germany

8

9 **Corresponding author**

10 Troy Ka-Yan Lui (kayan.lui@uni-luebeck.de)

11

12 **Competing interests**

13 The authors declare no conflict of interest.

14

15 **Data availability**

16 Raw data are available from the corresponding authors upon request. Pre-processed
17 behavioural and neural responses as a function of distractor onset time will be made available
18 online upon publication.

19

20 **Author contributions**

21 Conceptualization, T.K.L., J.O., and M.W.; methodology, T.K.L., J.O., and M.W.;
22 investigation, T.K.L. ; formal analysis, T.K.L., J.O., and M.W. ; writing – original draft, T.K.L.
23 and M.W.; writing – review & editing T.K.L., J.O., and M.W.; funding acquisition, M.W.

24

25 **Funding**

26 This work was supported by Deutsche Forschungsgemeinschaft [grant number WO 2371/1-1].

27

28 **Keywords**

29 attention; auditory; distractibility; distraction; rhythmic cognition; theta oscillations

30

Abstract

31 Human environments comprise various sources of distraction, which often occur unexpectedly
32 in time. The proneness to distraction (i.e., distractibility) is posited to be independent of
33 attentional sampling of targets, but its temporal dynamics and neurobiological basis are largely
34 unknown. Brain oscillations in the theta band (3–8 Hz) have been associated with fluctuating
35 neural excitability, which is hypothesised here to explain rhythmic modulation of distractibility.
36 In a pitch discrimination task ($N = 30$) with unexpected auditory distractors, we show that
37 distractor-evoked neural responses in the electroencephalogram and perceptual susceptibility
38 to distraction were co-modulated and cycled approximately 3–5 times per second. Pre-
39 distractor neural phase in left inferior frontal and insular cortex regions explained fluctuating
40 distractibility. Thus, human distractibility is not constant but fluctuates on a subsecond
41 timescale. Furthermore, slow neural oscillations subserve the behavioural consequences of a
42 hitherto largely unexplained but ever-increasing phenomenon in modern environments –
43 distraction by unexpected sound.

44

Introduction

45 Selective attention enables humans to focus on relevant information at the expense of
46 distraction. The brain prioritizes representations of relevant events while filtering out task-
47 irrelevant distractors (Desimone & Duncan, 1995; Picton et al., 1971). Recent research posited
48 that distractor processing is not merely collateral to attentional sampling of targets but may
49 follow its own dynamics (Schneider et al., 2018; Wöstmann et al., 2019, 2020). The
50 behavioural detriments induced by different kinds of distractors (i.e., *distraction*) and the
51 neuro-cognitive mechanisms that counteract distraction (i.e., *suppression*) have been studied
52 in some detail (Bonnefond & Jensen, 2012; Geng & DiQuattro, 2010; van Moorselaar et al.,
53 2020; Weisz et al., 2020; Wöstmann et al., 2019). However, the temporal dynamics and the
54 neurobiological basis of the proneness to distraction (i.e., *distractibility*) are largely unknown.

55 Distractibility has long been neglected in the theoretical formulation of rhythmic
56 attention. Originally assumed to be static (Posner et al., 1980), the attentional spotlight was
57 proposed to be blinking at a subsecond time scale in a theta-like rhythm (i.e., 3–8 Hz)
58 (Buschman & Kastner, 2015; Fiebelkorn & Kastner, 2019). Behaviourally, it is manifested via
59 the waxing and waning of behavioural performance in target selection (Fiebelkorn et al., 2013;
60 Ho et al., 2017; Kubetschek & Kayser, 2021; Landau & Fries, 2012) or working memory
61 (Schmid et al., 2022; ter Wal et al., 2021) performance at similar frequencies. However, the
62 temporal dynamics outside of the attentional spotlight are not well understood. While previous
63 research studied how distractibility unfolds on relatively long temporal scales of minutes (i.e.,
64 during an experimental session (Forster & Lavie, 2014)) or years (i.e., across stages of
65 development (Campbell et al., 2012; Kannass et al., 2006)), we found preliminary evidence for
66 fluctuating distractibility on shorter timescales following rhythmic presentation of auditory
67 targets (Wöstmann et al., 2020). To isolate distractibility dynamics from rhythmic entrainment
68 or preparatory suppression, we here employ a design that uses non-rhythmic stimuli and
69 distractors that occur unexpectedly.

70 A central prediction of rhythmic attention is that the phase of slow neural oscillations
71 explains fluctuations in behaviour (VanRullen, 2016). The prediction is based on the notion
72 that rhythmic attention arises from the periodic excitability of the attention-related brain
73 network (Fiebelkorn & Kastner, 2019; VanRullen, 2016). In the human brain, theta neural
74 phase (3–8 Hz) is assumed to reflect moment-to-moment changes in neural excitability
75 (Lakatos et al., 2005). Theta phase in brain regions beyond sensory cortices, such as fronto-

76 parietal regions and the hippocampus, has been associated with fluctuations in target detection
77 (Helfrich et al., 2018) and working memory encoding (Rutishauser et al., 2010; Siegel et al.,
78 2009), respectively. While previous research has related distractibility to supra-modal regions
79 in frontal (Chao & Knight, 1995; Wais et al., 2012) or parietal (Kanai et al., 2011) cortex, it is
80 unclear whether and in which networks the momentary neural dynamics may subserve the
81 waxing and waning of distractibility.

82 Here, we ask if the brain spontaneously alternates between states of higher and lower
83 distractibility and whether such fluctuations have the potency to explain behavioural
84 consequences of distraction. If so, we would expect to observe a brain-behaviour relation
85 between the pre-distractor brain state and the distractor-induced detriment in task performance.
86 To this end, we employed a pitch discrimination task wherein an auditory distractor could occur
87 at variable and unexpected times in-between two target tones. A total of 17,280 behavioural
88 and neural responses in the electroencephalogram (EEG) in N=30 participants revealed that
89 behavioural sensitivity and distractor-evoked neural responses fluctuated in sync across
90 distractor onset times in ~3–5 cycles per second. Critically, pre-distractor theta phase in left
91 inferior frontal and insular cortex regions explained behavioural performance fluctuations.
92 These effects were absent in trials without distractors, reinforcing their specificity to distractor-
93 related neural processing.

94

Material and Methods

95 Participants

96 Thirty participants (20 females, 10 males; mean age = 23.67, SD = 3.56) took part in the EEG
97 experiment. They provided written informed consent and were compensated by either €10/hour
98 or course credit. Participants were right-handed according to the Edinburgh Handedness
99 Inventory (Oldfield, 1971) (mean score = 92), with self-reported normal hearing, normal or
100 corrected-to-normal vision, and no psychological or neurological disorders. All procedures of
101 the current study were approved by the ethics committee of the University of Lübeck.

102 Stimuli and Procedure

103 Participants performed a pitch discrimination task wherein they decided whether the first (tone
104 1) and the second (tone 2) target tones in a trial were the same or different in pitch. Prior to the
105 experiment, they were instructed to answer as accurately and as fast as possible. The target
106 tones were 75 ms long pure tones with 5 ms rise and fall periods. In each trial, the frequencies
107 of tone 1 were randomly selected between musical note A#3 (233 Hz) and G#5 (830.6 Hz),
108 while that of tone 2 was either the same (50%) or different (higher or lower, 25% each) in
109 frequency compared to tone 1.

110 The pitch difference between tone 1 and tone 2 was titrated for each participant with an
111 adaptive task (see below). The offset-to-onset interval between tone 1 and tone 2 was 1550 ms.
112 Each distractor stimulus comprised 10 consecutive pure tones with 40 ms duration (400 ms in
113 total). The frequencies of the pure tones in each distractor stimulus were randomly selected
114 among the 12 tones between A#3 and G#5 with whole tone steps (A#3, C4, D4, E4, F#4, G#4,
115 A#4, C5, D5, E5, F#5, and G#5), with the constraint that there would be no repetition between
116 consecutive tones. Each of the 12 tone frequencies appeared at each of the 10 positions with
117 equal probability across trials.

118 In-between the two target tones, a distractor was presented in 50% of trials (distractor-
119 present condition) and no distractor was presented in the remaining trials (distractor-absent
120 condition). In the distractor-present condition, the distractor was presented at one of 24
121 distractor onset times (0 ms to 1150 ms, 50-ms steps, relative to the offset of tone 1), which
122 was selected at random on each trial. After the offset of target tone 2, participants had a 2000
123 ms response time window. To avoid potential temporal predictability effects of the onset of the

124 next trial, the inter-trial intervals were randomly selected from a truncated exponential
125 distribution (mean = 1460 ms), ranging between 730 and 3270 ms.

126 The trial order was pseudo-randomized with no repetition in probe tone frequency and
127 distractor onset for any two consecutive trials. In total, there were 12 trials for each unique
128 condition (distractor-present/absent x distractor onset x same/different target pitch) and 1152
129 trials for the whole experiment. All auditory materials were presented via Sennheiser
130 headphones (HD 25-1 II). Responses were made using a response box (The Black Box Toolkit).
131 The assignment of buttons to the response options (“same” or “different”) was counterbalanced
132 across participants. Stimuli were presented via Matlab (MathWorks, Inc., Natick, USA) and
133 Psychtoolbox(Brainard, 1997). The auditory stimuli were presented at approximately 70 dB
134 SPL.

135 **Adaptive Staircase Procedure**

136 Prior to the main experiment, each participant’s threshold for the pitch discrimination task was
137 titrated using an adaptive staircase procedure, implemented in the Palamedes toolbox (Prins &
138 Kingdom, 2018) for Matlab. For the initial 11 participants, the threshold was titrated to an
139 approximate accuracy of 70.7%. As the overall accuracy was relatively high even after the
140 adaptive staircase procedure for these 11 participants (mean = 79.59%, SD = 10.43%), the final
141 16 participants performed an adaptive procedure altered to yield approximately 65% accuracy
142 instead. Due to technical issues, performance of the remaining three participants was tracked
143 at 35% accuracy. As all relevant statistical analyses in the present study are within-subject, and
144 as paired t-tests (2-tailed) comparing the behavioural performance between distractor-absent
145 and distractor-present conditions were significant with ($t_{29} = 8.11, p < .001$) and without ($t_{26} =$
146 $9.41, p < .001$) these participants, their data were included in the final analysis.

147 Each participant went through the adaptive staircase procedure two to three times,
148 depending on the stability of the tracked threshold. There were in total 30 trials for each run of
149 the adaptive staircase procedure with an initial pitch difference of 100 cents (i.e. 1 semitone)
150 between tone 1 and 2. The minimum and maximum pitch difference possible in the task was 2
151 cents and 2000 cents, respectively. For the procedure which tracked performance at ~70.7%, a
152 two-down one-up procedure was used. Specifically, the pitch differences would decrease in
153 steps of 10 cents if participant responded correctly (i.e., different), or increase in steps of 10
154 cents if participant responded incorrectly (i.e., same) for 2 consecutive trials. For the procedure

155 which tracked performance at ~65% procedure, the pitch differences would decrease in steps
156 of 7 cents if participant answered correctly or increase in steps of 13 cents if they answered
157 incorrectly. The pitch difference used in the main experiment was calculated by averaging the
158 final 10 trials in the tracking run which converged to the most stable threshold, determined by
159 visual inspection, in the ~70.7% procedure. The same procedure was used to average the final
160 6 trials in the ~65% procedure. Overall accuracy averaged across all participants in the actual
161 experiment was 73.58% (SD = 12.12%).

162 **Behavioural Data Analysis**

163 To understand how distractors affect pitch discrimination performance in the framework of
164 signal detection theory, we calculated sensitivity (d') and criterion (c) separately for distractor-
165 present and -absent conditions, using the Palamedes toolbox (Prins & Kingdom, 2018) and the
166 following formulas:

167 (Formula 1)
$$\text{Sensitivity} = z(\text{Hit rate}) - z(\text{False alarm rate})$$

168 (Formula 2)
$$\text{Criterion} = -0.5 * (z(\text{Hit rate}) + z(\text{False alarm rate}))$$

169 Hit rate was defined as the “different” response when the two tones were different in
170 pitch, and false alarm rate the “different” response when the two tones were the same in pitch.
171 Extreme values (0 or 1) of Hit rate or False alarm rate were adjusted (Macmillan & Kaplan,
172 1985): A rate of 0 was adjusted by dividing 1 by the number of trials multiplied by 2; while a
173 value of 1 was adjusted by subtracting the same value from 1. Paired samples t-tests (2-tailed)
174 were used to compare sensitivity and criterion in distractor-present versus -absent conditions.

175 To study the modulation of distractor onset times on behavioural measures in the
176 distractor-present condition, sensitivity for each distractor onset time was calculated, resulting
177 in a behavioural time course as a function of distractor onset time for each individual participant
178 (see Fig. S1 & S2).

179 **EEG Recording and Pre-processing**

180 The experiment was conducted in an electrically shielded sound-attenuated room. A modified
181 10-20 international system with 64 Ag/Ag-Cl electrodes was used to record the EEG with a
182 sampling rate of 1000 Hz (actiCHamp, Brain Products, München, Germany). The EEG
183 recordings were band-pass filtered online from direct current (DC) to 280 Hz. TP9 was used

184 as the online reference and FPz as the ground electrode. Impedances were kept below 20 kOhm
185 for all but one participant.

186 Matlab R2018a (MathWorks, Inc., Natick, USA) and the Fieldtrip toolbox (Oostenveld
187 et al., 2011) were used to pre-process and analyse EEG data. The continuous EEG data were
188 filtered (high-pass, 1 Hz; low-pass, 100 Hz) before they were segmented into epochs (-2 to
189 2.5s) time-locked to tone 1 onset. Independent component analysis (ICA) was used to identify
190 and reject components corresponding to artefacts such as eye blinks, eye movements, and
191 muscle activity (average percentage of components removed = 26.46%, SD = 8.89%).
192 Afterwards, EEG data were re-referenced to the average of all electrodes. Epochs with
193 amplitude changes >160 microvolts were rejected (average percentage of epochs removed =
194 1.35%, SD = 2%).

195 To obtain distractor-evoked neural responses, data were re-epoched to the onset of the
196 distractor (-1 to 1 s) with a 200ms baseline period. Epochs belonging to the same conditions
197 (distractor-present/absent) and distractor onset time (0 – 1150ms, 50-ms steps) were then
198 averaged into ERP waveforms. The spectral amplitude of distractor-evoked responses at 25 Hz,
199 which corresponds to the temporal structure of the distractor, was extracted using FFT on the
200 ERP waveform in the time window from 0 to 520ms after distractor onset. Spectral amplitude
201 was averaged across electrodes F1, Fz, F2, FC1, FCz, and FC2. For each participant, the 24
202 spectral amplitudes, corresponding to the 24 distractor onset times, resulted in a neural time
203 course of distractor processing as a function of distractor onset time (see Fig. S1 & S2).

204 Distractor-evoked inter-trial phase coherence (ITPC) was also calculated across
205 frequencies (1 – 10 Hz, 1-Hz steps) and time windows (-0.2 – 0.7 s, 0.05-s steps) for each
206 electrode. First, Fourier coefficients were calculated (using windows with a fixed length of 0.5
207 s; hanning taper). Then, the complex Fourier coefficients were divided by their magnitude and
208 averaged across trials. ITPC was calculated by taking the absolute value (i.e., magnitude) of
209 the average complex coefficient.

210 **Modulation of neural and behavioural measures by distractor onset time**

211 To test whether and how distractor onset time modulates neural and behavioural measures, we
212 used linear mixed-effect models with sine- and cosine-transformed distractor onset time,
213 similar to Wöstmann et al. 2020 (Wöstmann et al., 2020). For time courses of sensitivity and
214 spectral amplitude of the distractor-evoked ERP at 25 Hz separately, we first subtracted the

215 individually fitted quadratic trend (computed with the polyfit function in Matlab) from the
216 original time course for each participant (see Fig. S1 & S2) as the quadratic trend was not of
217 interest in the current study (Huang et al., 2015).

218 Then, we designed sine- and cosine- transformed distractor onset time vectors using the
219 following formulas,

220 (Formula 3) Sine predictor = $\sin(2 * \pi * f * \text{distractor onset time})$

221 (Formula 4) Cosine predictor = $\cos(2 * \pi * f * \text{distractor onset time})$

222 Where f denotes the frequency of interest (0.5 – 8 Hz, 0.5-Hz steps). Next, we regressed the
223 detrended sensitivity and spectral amplitude of ERP time courses on sine and cosine predictors
224 using linear mixed models (using the fitlme function in Matlab) for each frequency of interest
225 using the following formulas:

226 (Formula 5) $z(\text{sensitivity}) \sim z(\text{sine predictor}) + z(\text{cosine predictor}) + (1|\text{participant})$

227 (Formula 6) $z(25\text{-Hz ERP}) \sim z(\text{sine predictor}) + z(\text{cosine predictor}) + (1|\text{participant})$

228 Spectral magnitude for each frequency was computed by taking the square root of the sum of
229 squared beta coefficients of sine and cosine predictors:

230 (Formula 7) Spectral magnitude = $\sqrt{(\text{sine coef}^2 + \text{cosine coef}^2)}$

231 Statistical significance of the spectral magnitude was determined by comparing the
232 spectral magnitude of the empirical data with the 95th percentile of a permutation distribution,
233 which was generated by shuffling the original behavioural/neural time course and performing
234 the same analysis for 5,000 times.

235 To test whether sensitivity and spectral amplitude of the distractor-evoked ERP at 25
236 Hz are co-modulated, for each participant, cross-correlation coefficients across time lags of the
237 two signals were obtained (using the “xcorr” function on z-scored time courses in Matlab).
238 Again, we ran a similar linear mixed model as explained above, but this time with sine- and
239 cosine- transformed time lags as predictors and used the correlation coefficients from the cross-
240 correlation as the outcome measure. Spectral magnitude was obtained using formula 7 and
241 statistical significance with the same permutation method mentioned above.

242 **Phasic modulation of behavioural sensitivity**

243 To explore the role of pre-distractor neural dynamics on the pitch discrimination performance,
244 we examined whether pre-distractor oscillatory phase relates to behavioural sensitivity. To this
245 end, we examined the quadratic fit of sensitivity as a function of neural phase in source space.

246 First, we implemented the source analysis using the Fieldtrip toolbox. First, a standard
247 volume conduction model and standard electrode locations were used to calculate the leadfield
248 matrix with 10-mm resolution. We applied the linearly constrained minimum variance (Van
249 Veen et al., 1997) (LCMV) beamformer approach on the 10 Hz lowpass filtered data centred
250 around distractor onset (-1 to 1s). We calculated a common filter including all trials by
251 calculating the covariance matrix estimates. There were in total 2,015 source locations inside
252 the brain.

253 Second, a quadratic fit analysis resolved by frequency and time probed the spectral and
254 temporal specificity of the phasic modulation of perceptual sensitivity. To obtain trial-wise
255 phase values for each source location, the following procedure was implemented for each trial
256 in each source location: First, the single-trial EEG time course was projected into the source
257 space using the common filter. Then, a sliding window (0.4s duration; moving in 50-ms steps
258 from -0.3 to +0.3s relative to distractor onset) was employed to transform the data into the
259 frequency domain (using FFT). Note that the time point of the sliding window refers to the
260 mid-point of each time window. For instance, the time window centred at -0.3 included data
261 from -0.5 to -0.1 s. The respective phase value of each frequency (2.5 – 8 Hz in 0.5-Hz steps)
262 was then calculated using the *angle* function in MATLAB. The phase values of all trials were
263 binned into 9 bins of equal size, ranging from -pi to pi, followed by a calculation of sensitivity
264 for each bin. The quadratic fit of sensitivity across phase bins was estimated using the *polyfit*
265 function (order = 2) in MATLAB. As a result, we obtained a quadratic fit index for each source
266 location, frequency, and time of interest.

267 We used a source-level cluster-based permutation test (Maris & Oostenveld, 2007) to
268 find significant clusters in voxel-frequency-time space that would exhibit phasic modulation
269 of sensitivity. Dependent-samples t-tests were used to contrast quadratic fit coefficients against
270 zero, followed by clustering of adjacent bins with significant effects in voxel-frequency-time
271 space. To derive cluster p-values, summed t-values in observed clusters were tested against
272 5,000 permutations with shuffled condition labels (two-tailed).

273 To demonstrate that the significant cluster found in the above analysis does not
274 primarily originate from auditory cortex, we localised, for comparison, the distractor-evoked
275 inter-trial phase coherence (ITPC) at 3 – 7 Hz, strongly assumed to emerge at least to large
276 degrees from the supratemporal plane and auditory cortex (Koerner & Zhang, 2015; Mayhew
277 et al., 2010; Oya et al., 2018), with the following procedure for each voxel: For each trial, we
278 projected the time series EEG data into source space using the same common filter as in the
279 analysis on the phasic relationship with behaviour. Then, we transformed the source-projected
280 data (0 – 300 ms after distractor onset) to the frequency domain using FFT. The same
281 calculation as on the sensor level was used to calculate the ITPC for each frequency. ITPC
282 across frequencies 3 – 7 Hz were then averaged to obtain one distractor-evoked ITPC value for
283 each voxel.

284

285

286

Results

287 In the current electroencephalography (EEG) and behavioural study, we aimed at (1)
288 uncovering the temporal fluctuations in distraction, and (2) exploring the relationship between
289 such fluctuations and momentary neural phase at similar frequencies. To this end, we varied
290 the onset time of an auditory distractor that was presented in-between two to-be-compared
291 tones in a variant of a pitch discrimination task.

292 We probed this research question in the auditory modality as temporal information is
293 especially important to auditory attentional selection (Shamma et al., 2011). During the task,
294 participants ($N = 30$) had to identify whether the two target tones were the same or different in
295 pitch (Fig 1A). The distractor was a fast-varying, 25-Hz modulated sequence of tones that
296 differed in pitch, which allowed us to extract its induced 25-Hz neural response (Ding & Simon,
297 2009).

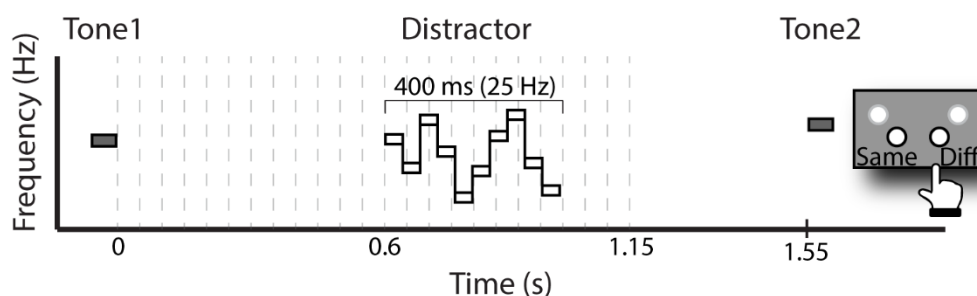
298 Distractors were present in half of the trials and absent in the remaining trials. In
299 distractor-present trials, the distractor onset was uniformly distributed across 24 onset times (0
300 – 1.15 s, in 0.05 s steps, after tone 1 offset). In distractor-absent trials, no distractor was
301 presented between the two tones. The inclusion of distractor-absent trials serves two purposes.
302 First, we could verify that the distractors had the potency to distract by comparing behavioural
303 performance for distractor-present versus distractor-absent trials (Wöstmann et al., 2022).
304 Second, participants could not anticipate whether or when a distractor would occur in a given
305 trial, which eliminated potential effects of such anticipation on behavioural performance
306 (Grabenhorst et al., 2021) or pre-stimulus neural activity (Dürschmid et al., n.d.; Herbst et al.,
307 2022; Stefanics et al., 2010).

308 **Distractors interfere with pitch discrimination performance**

309 To examine the potency of the distractors to distract, we compared participants' sensitivity and
310 criterion (response bias) of the pitch discrimination task between distractor-present and -absent
311 trials. Participants were less sensitive to the pitch difference ($t_{29} = -8.11, p = <.001$, Cohen's d
312 = -1.48), and had a more conservative response criterion (i.e., more "same pitch" responses; t_{29}
313 = 2.83, $p = .008$, Cohen's $d = 0.52$) on distractor-present trials (Fig 1B).

A

Schematic of a distractor-present trial



B

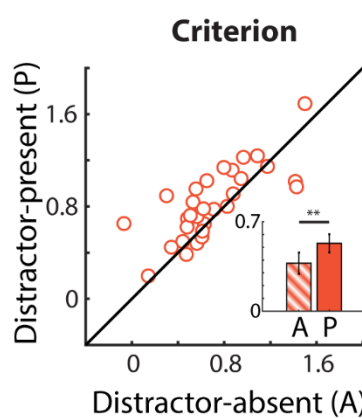
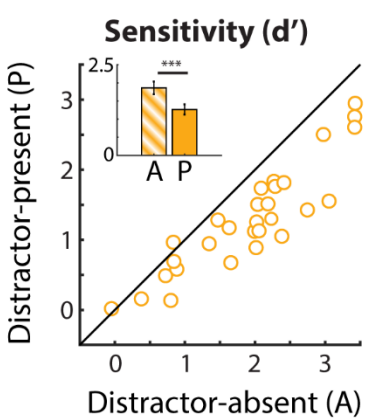


Fig 1. Experimental design and behavioural results.

316 A) Schematic of a distractor-present trial. Participants were instructed to indicate whether the two target tones (grey) were
317 the same (probability = 50%) or different (higher, probability = 25%; or lower, probability = 25%) in pitch. A 10-tone-pip
318 distractor sequence (white) with a 25-Hz temporal structure (i.e., 40-ms tone-pip duration; total duration 400 ms) was presented
319 at one of the 24 distractor onset times (dashed lines). In distractor-absent trials, no distractor was presented. B) Behavioural
320 results comparing distractor-present and -absent conditions. Coloured circles indicate single-subject data. Insets show bar
321 graphs of perceptual sensitivity (left panel) and criterion (right panel) for distractor-present (solid bar) and distractor-absent
322 (gradient bar) conditions, respectively. Error bars show ± 1 SEM. ** $p < .01$. *** $p < .001$.

323

324 **Behavioural and neural measures of distraction co-fluctuate across time**

325 Does the impact of distraction on neural activity and goal-directed behaviour exhibit
326 fluctuations across time? To test this, we varied distractor onset time and examined whether
327 behavioural and neural measures of distraction would show modulations at frequencies up to 8
328 Hz. Behaviourally, perceptual sensitivity was calculated as an indirect measure of distraction:
329 The more distracted, the lower the sensitivity in pitch discrimination should be (Fig 2A, yellow,
330 see S1 Fig for individual participants' time courses). Neurally, we calculated the distractor-
331 evoked event-related potential (ERP; Fig 2B) for each distractor onset time and used a fast
332 Fourier transform (FFT) to extract its amplitude at 25 Hz, which corresponded to the
333 modulation rate of the frequency-modulated distractor tone sequence (Fig 2A, blue, see S1 Fig
334 for individual participants' time courses).

335 To examine temporal fluctuations of distraction, we used linear mixed-effects models
336 with sine- and cosine- transformed distractor onset time as predictors to model behavioural (i.e.,
337 perceptual sensitivity) and neural (i.e., distractor-evoked ERP) time courses as the outcome
338 measures. This method outperforms other methods for studying the phasic modulation of
339 behavioural and neural responses (Zoefel et al., 2019) and has also been used previously
340 (Wöstmann et al., 2020) to extract temporal fluctuations in the vulnerability of working
341 memory to distraction. A quadratic trend was observed in the behavioural time course in Fig
342 2A as the earliest and latest distractors were most distracting due to their temporal proximity
343 to the target tones. Before running linear mixed models, we removed the quadratic trends in
344 the two measures as they were not of interest in the current study (Huang et al., 2015).

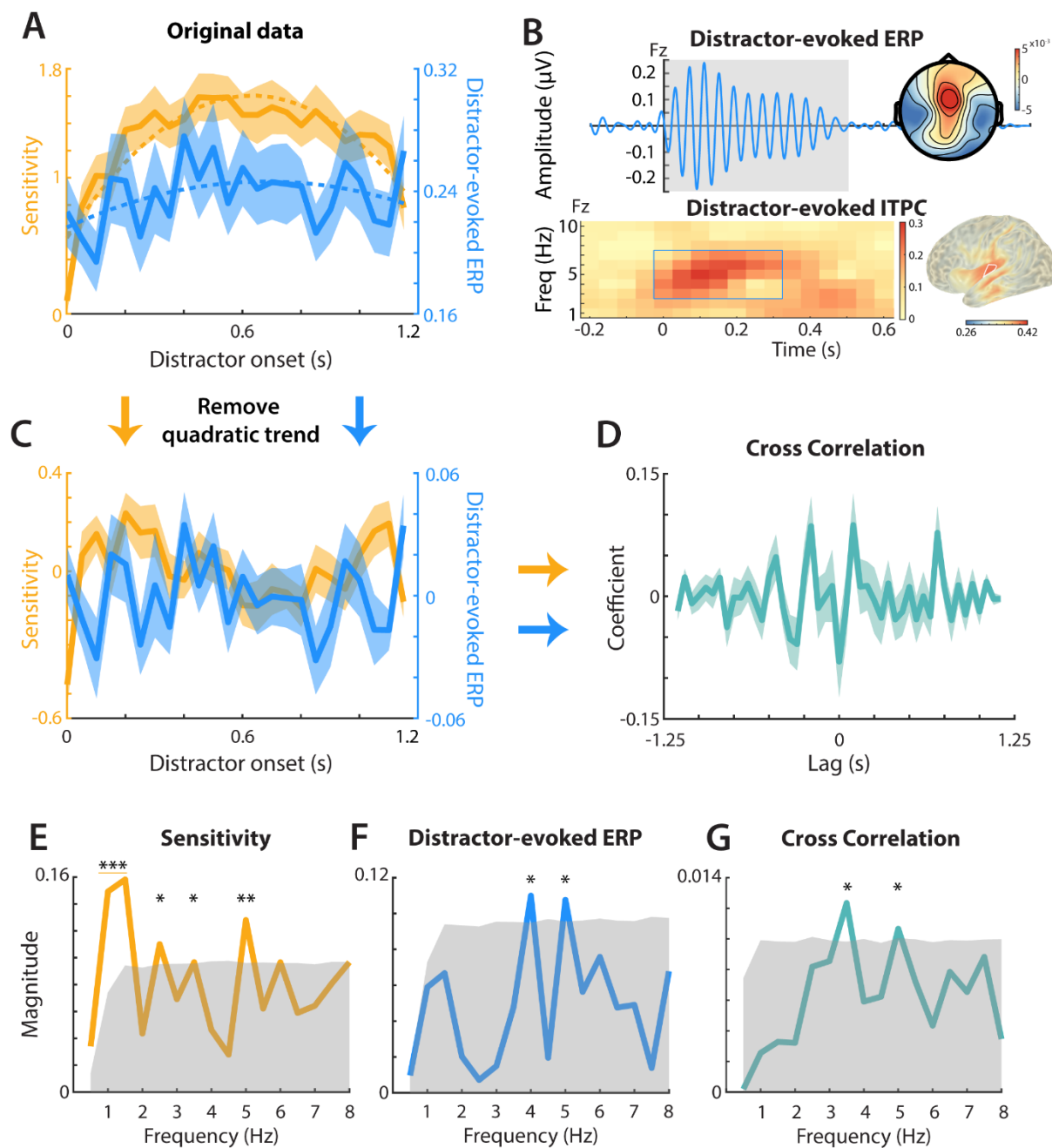
345 Fig 2E and F show the spectral magnitude (0.5–8 Hz, 0.5-Hz steps) resulting from linear
346 mixed models on detrended perceptual sensitivity (Fig 2C, yellow) and detrended ERP
347 amplitude (Fig 2C, blue), respectively. Statistical significance was derived by testing empirical
348 spectral magnitude against the 95th percentile of a permutation distribution, which was derived
349 from shuffling the behavioural and neural time courses, respectively, 5,000 times (see Methods
350 for details).

351 At the behavioural level, distractor onset time modulated sensitivity below 5 Hz. At the
352 neural level, distractor onset time modulated the distractor-evoked ERP at 4 and 5 Hz. Similar
353 results were obtained in a control analysis, where temporal fluctuations in sensitivity in
354 distractor-present trials were compared against distractor-absent trials (instead of permuted
355 distractor-present trials; S3 Fig).

356 If these periodic neural dynamics serve as the basis for the apparent behavioural
357 fluctuations, we should observe the synchronization of the behavioural and neural time courses
358 by a common rhythm. To test this, we also examined the co-modulation of sensitivity and
359 distractor-evoked ERP by distractor onset time. We first calculated the cross-correlation
360 coefficients of the behavioural and neural time courses for individual participants (Fig 2D). We
361 then ran a linear mixed model with the cross-correlation coefficient as the outcome measure
362 and sine- and cosine-transformed time lag as predictors.

363 Fig 2G shows that sensitivity and distractor-evoked ERP are co-modulated at 3.5 and 5
364 Hz. At lag 0, there was a negative correlation between sensitivity and the distractor-evoked
365 ERP, consistent with the notion that stronger distractor encoding (i.e., larger distractor-evoked
366 ERP) corresponds to worse task performance (i.e., lower sensitivity). T-tests against zero on
367 the (Fisher-z transformed) correlation coefficients across participants show that this correlation
368 at time lag 0 was close to statistical significance (Pearson's r : $t_{29} = -1.85$, $p = 0.08$, mean
369 Pearson's $r = -0.08$; Spearman's r : $t_{29} = -2.13$, $p = 0.04$, mean Spearman's $r = -0.10$).

370 As a control analysis, the same analysis pipeline was run on the data in the distractor-
371 absent condition by randomly assigning a “distractor onset” for each distractor-absent trial,
372 which did not reveal any significant co-modulation (S4 Fig): Neither time courses of sensitivity
373 nor distractor-evoked ERP were modulated by distractor onset time; time lags did not modulate
374 the cross-correlation of these two at any frequency. The temporal co-fluctuations of
375 behavioural and neural measures of distraction at 3 – 5 Hz in distractor-present trials may be a
376 manifestation of an underlying distractibility rhythm, which we probed into next.



377

378 **Fig 2. The analyses of behavioural and neural time courses by distractor onset time.**

379 A) Average sensitivity (yellow solid line) and 25-Hz amplitude of the distractor-evoked event-related potential (ERP; blue
 380 solid line) across distractor onset times. Shaded areas show ± 1 SEM across participants. Dashed lines show respective
 381 quadratic trends. B) Top panel: Distractor-evoked ERP waveform averaged across all distractor onset times at electrode Fz
 382 (20 – 30 Hz bandpass filtered for visualization purpose). Shaded grey area marks the time window used to extract the 25-Hz
 383 amplitude of the distractor-evoked ERP. Inset shows the scalp map of the 25-Hz amplitude of the distractor-evoked ERP
 384 (derived via an FFT on the distractor-evoked ERP waveform). Bottom panel: Distractor-evoked inter-trial phase coherence
 385 (ITPC) from 1 – 10 Hz and from -0.2 s – 0.6 s at Fz. Brain surface shows the ITPC values (frequencies: 3 – 7 Hz; time window:
 386 0 – 0.3 s) in source space, which reflects the auditory response to the distractor. White outline indicates top 1% voxels with
 387 largest ITPC values. C) Detrended time courses of behavioural and neural outcome measures. Shaded areas show ± 1 SEM
 388 across participants. D) Solid line shows average correlation coefficients, derived by averaging single-subject cross-correlations

389 of sensitivity and distractor-evoked ERP time courses, as a function of temporal lags. Shaded area shows ± 1 SEM across
390 participants. E-G) Spectral magnitude across frequencies (0.5 – 8 Hz, 0.5-Hz step) for (E) detrended sensitivity, (F) distractor-
391 evoked ERP, and (G) the cross-correlation between the two. Shaded areas show the 95th percentile of the permutation
392 distribution generated from 5,000 permutations. * $p < .05$. ** $p < .01$. (uncorrected)

393

394 **Pre-distractor neural phase in inferior frontal/insular cortex explains distraction**

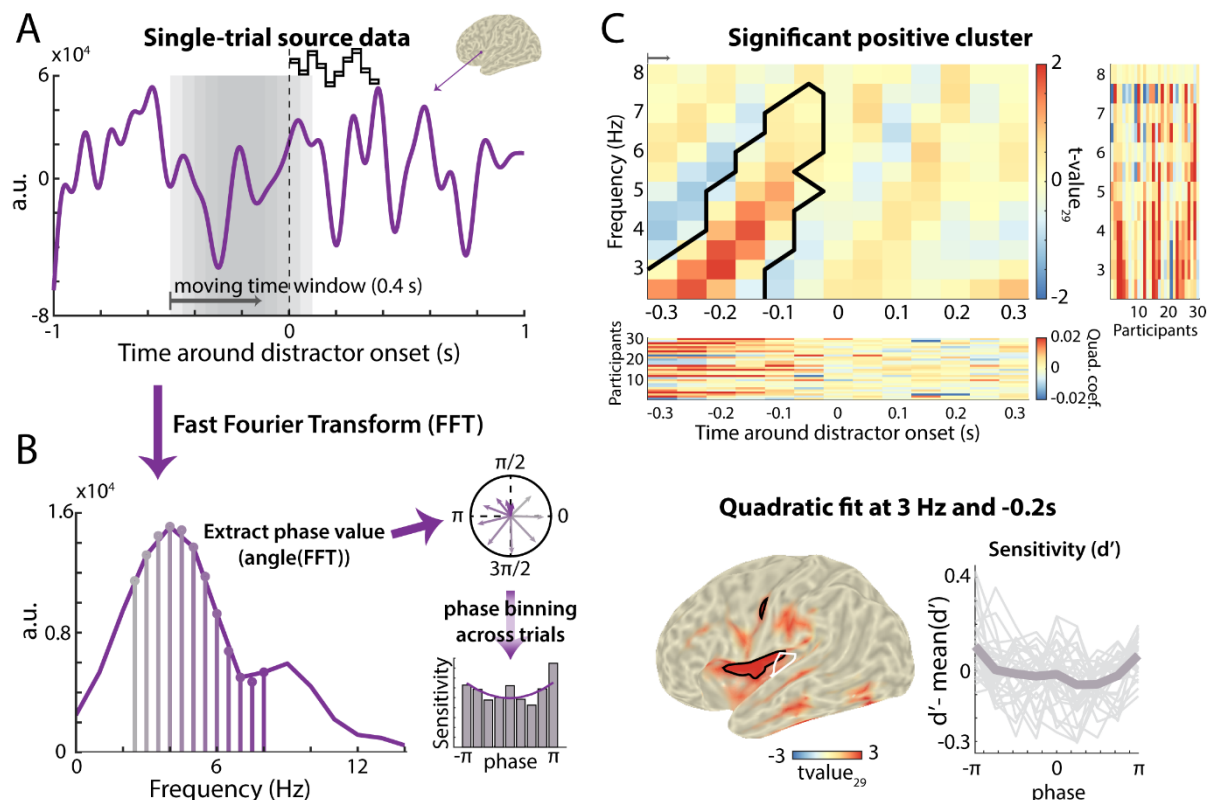
395 If the human brain hosts an endogenous rhythm that underlies distractibility dynamics, the
396 neural state prior to distractor onset should explain the participant's momentary vulnerability
397 to interference by a distractor. To test this, we studied how pre-distractor neural phase relates
398 to our previously established proxy of distraction, that is, behavioural sensitivity. We asked
399 when in time and in which brain network(s) such an endogenous rhythm underlying
400 distractibility would show up.

401 We employed source-projected EEG time courses to extract the quadratic relationship
402 between the binned pre-distractor neural phase and perceptual sensitivity. For each trial (Fig
403 3A), we first transformed a source-projected EEG data segment (0.4 s; sliding window) into
404 the frequency domain using FFT. We then extracted neural phase for a given frequency (Fig
405 3B). To calculate sensitivity sorted by phase bin, we first sorted the trials according to their
406 phase values into 9 phase bins of equal size, followed by calculation of perceptual sensitivity
407 for each bin (see S5 Fig for individual participants' sensitivity by phase bin). The same
408 procedure was repeated for a range of frequencies (2.5 – 8 Hz, 0.5-Hz steps) and time windows
409 (-0.3 – 0.3 s around distractor onset, 0.05-s steps). A cluster-based permutation test with the
410 dimensions time, frequency, and voxels, wherein the quadratic fit was tested against zero,
411 revealed a positive significant cluster (Fig 3C; the same analyses with 7, 8, and 10 phase bins
412 yielded comparable clusters across all dimensions and comparable statistical significance). The
413 quadratic modulation of sensitivity by neural phase at 2.5 – 7.5 Hz was most prominent in the
414 left insular and the inferior frontal cortices in the time window spanning ~300 ms before
415 distractor onset (cluster p -value = .026, two-tailed; see S6 Fig for brain surface plots from other
416 viewing angles).

417 To test whether the significant cluster overlaps with sources of auditory-evoked activity
418 in auditory cortex regions, we compared its source with the source of distractor-evoked inter-
419 trial phase coherence (ITPC) at 3 – 7 Hz (shown also in Fig 2B, bottom panel). Importantly,

420 although the two effects were localized in proximal cortical regions (Fig 3C, bottom panel),
 421 their core regions were mostly non-overlapping.

422 For control, we conducted the same analysis on the distractor-absent trials, which
 423 revealed no significant cluster (S7 Fig). We also tested the relationship between the pre-
 424 distractor neural phase and the post-distractor neural measure of distraction (i.e., 25-Hz
 425 amplitude of the distractor-evoked ERP), which did not reveal a significant effect (S8 Fig).



426 **Fig 3. Cluster-based permutation test results on the relationship between neural phase and behavioural fluctuations.**

427 **Fig 3. Cluster-based permutation test results on the relationship between neural phase and behavioural fluctuations.**

428 A-B) Illustration of the source-level analysis. A) Example of a single-trial source-projected EEG time course. The moving
 429 window (grey) was used to transform segments of the data into the frequency domain using FFT. The first grey window
 430 corresponds to the first time window used in the time-resolved analysis (i.e., -0.5 to -0.1 s). B) Spectral representation of the
 431 data segment in (A). Phase values across frequencies were extracted and trials were binned according to their phase values
 432 into 9 phase bins for each frequency, time window, and source location. Bar graph shows exemplary sensitivity values
 433 calculated from the trials sorted by phase bin. A quadratic trend was fitted to the sensitivity values across phase bins (purple
 434 solid line). C) Results of a cluster-based permutation test, which tested quadratic fits in time-frequency-source space against
 435 zero. Top panel shows the t-values (df = 29) across frequencies and time windows, averaged across all the voxels belonging
 436 to the significant positive cluster. The black contour indicates the positive significant cluster. Right column shows individual
 437 participants' quadratic coefficients for each frequency, collapsed across the time windows included in the significant cluster.
 438 Bottom row shows individual participants' quadratic coefficients across time windows, collapsed across frequencies and
 439 voxels included in the significant cluster. Bottom left panel shows the cluster peak effect (3 Hz; -0.2 s), which resides mainly
 440 in left inferior frontal cortex and insular cortex. Only the t-values of the positive significant cluster are shown. The black
 441 contour indicates the regions with the top 1% t-values across the whole brain. The t-values were interpolated and projected

442 onto MNI coordinates for visualization purposes. The white contour indicates distractor-evoked neural activity, quantified as
443 the top 1% inter-trial phase coherence (ITPC) in the post-distractor time window (i.e., 0 – 0.3 s) at 3 – 7 Hz (shown also in
444 Figure 2B). Bottom right panel shows centred perceptual sensitivity sorted by phase bins in the positive cluster at 3 Hz averaged
445 across participants. Grey thin lines show individual centred perceptual sensitivity.

446

Discussion

447 The current study aimed to unravel the temporal dynamics of distractibility, using a pitch
448 discrimination task with auditory distractors. The eventual degree of distraction and the neural
449 processing of distractors were respectively quantified by distractor-evoked performance
450 detriments and neural responses in the human electroencephalogram (EEG). We made a series
451 of interesting observations.

452 First, the ~3 – 5 Hz fluctuations of behavioural sensitivity across distractor onset time
453 urged for the question whether the same fluctuations are observed in the human brain's
454 response to distractors. Consistently, we found that the distractor-evoked neural response
455 covaries with behavioural sensitivity at similar frequencies. Second, while behavioural
456 sensitivity and the distractor-evoked neural response might partly reflect post-perceptual
457 processes (such as distractor suppression), we asked whether the brain hosts an endogenous
458 oscillation that shapes the momentary state of distractibility. Confirming this, we found that
459 pre-distractor neural phase in left inferior frontal/insular cortex explained rhythmic fluctuations
460 in the momentary degree of distraction.

461 These major findings support the notion that temporal fluctuations in distractibility on
462 a subsecond time scale can be explained by slow neural oscillatory dynamics in a cortical
463 network beyond the auditory cortex.

464 The proneness to distraction is inherently dynamic

465 The current study sheds light on the dynamics of distractibility, which is an important factor
466 often neglected in previous attention research on distraction and suppression. The ultimate
467 degree of detriment that a distractor will cause depends on two endogenous factors: the
468 momentary proneness to distraction (i.e., distractibility) and the ability to suppress a distractor
469 (i.e., distractor suppression). On the one hand, research on distractor suppression often did not
470 disentangle the active suppression of distractors (Schneider et al., 2021) from variations in
471 distractibility. On the other hand, research on distractibility rather treated it as an individual
472 characteristic that, if at all, only changes on a slow temporal scale such as within an
473 experimental session (Forster & Lavie, 2014) or across developmental stages (Kannass et al.,
474 2006). The temporal trajectory of distractibility on a faster, subsecond, time scale had hitherto
475 been left unknown.

476 With distractor-evoked behavioural and neural measures, we were able to encapsulate
477 the temporal trajectory of distraction, which fluctuates on a subsecond temporal scale
478 consistent with the rate of rhythmic sampling in attention (Fiebelkorn et al., 2013; Ho et al.,
479 2017; Kubetschek & Kayser, 2021; Landau & Fries, 2012) and working memory (Cruzat et al.,
480 2021; Schmid et al., 2022; ter Wal et al., 2021). With analysis of pre-distractor neural
481 oscillatory phase, we were able to trace this distractibility back to a slow neural oscillatory
482 fluctuation in inferior frontal and insular cortex (see below for an in-depth discussion).
483 Participants could not anticipate whether or when the distractor would occur, thereby not being
484 able to engage in preparatory suppression of the upcoming distractor (Geng, 2014). The
485 combined analysis of pre-distractor neural phase and of post-distractor neural and behavioural
486 measures complementarily elucidates how the brain alternates between states of higher and
487 lower distractibility. These insights are essential for the inclusion of an explicit account of
488 distraction in models of attention in psychology and neuroscience.

489 Fluctuations of distractibility at 3 – 5 Hz in the current study unveil the dynamic nature
490 of attention, which was underappreciated in the static spotlight metaphor of attention (Posner
491 et al., 1980). The attentional sampling of to-be-attended external stimuli (Fiebelkorn et al.,
492 2013; Ho et al., 2017; Kubetschek & Kayser, 2021) or internal memory representation (Cruzat
493 et al., 2021; Schmid et al., 2022; ter Wal et al., 2021) has been shown to exhibit temporal
494 fluctuations at similar frequencies. The waxing and waning of attentional sampling may index
495 inter-areal coordination between the attentional network and the sensory areas of the brain
496 (Dugué & VanRullen, 2017), which is associated with the alternation between stronger and
497 weaker attentional sampling over time (Fiebelkorn & Kastner, 2019). With much evidence on
498 the temporally dynamic nature of the attentional spotlight, however, there is a lack of
499 theoretical foundation for the inherent dynamics of cognition outside of this spotlight (Lui &
500 Wöstmann, 2022). With the observed fluctuations of distractibility in the theta frequency range,
501 an extension of the existing theory of dynamic attentional sampling to temporally dynamic
502 distraction is warranted.

503 While our results demonstrate that distractibility exhibits temporal fluctuations, they do
504 not reveal whether such fluctuations are independent of the fluctuations found in the attentional
505 sampling of memory content. Participants in the current study had to maintain the memory
506 representation of the pitch of tone 1 during a trial. The theta fluctuations found in the current
507 study thus may represent the sampling of the internal representation of tone 1, with higher
508 distractibility hypothetically occurring during the phase of reduced sampling of the memory

509 representation. Alternatively, observed theta fluctuations may represent independent
510 fluctuations in the proneness to distraction. Previous neuroimaging studies found that the
511 suppression of distracting inputs may be independent of the sampling of attended inputs
512 (Noonan et al., 2016; Schneider et al., 2018; Wöstmann et al., 2019). Future investigations may
513 manipulate both the target and distractor onset time to examine the relationship between the
514 temporal fluctuations underlying attentional sampling and distractibility.

515 Of note, as the main analysis approach used here (comparing empirical time courses to
516 time courses that were shuffled in time) does not distinguish between periodic and aperiodic
517 temporal structure (Brookshire, 2022), we are careful to conclude from the respective results
518 alone that distractibility is rhythmic. However, it does not negate the possibility that there is a
519 periodic temporal structure in distractibility. The premise of rhythmic cognition is that the
520 apparent fluctuations of performance reflect the periodic orchestration between brain regions
521 (Fiebelkorn & Kastner, 2019). In addition to fluctuations in behavioural performance, neural
522 evidence is therefore essential to elucidate the rhythmicity of cognition (Fiebelkorn, 2022;
523 Wöstmann, 2022). The current study shows a correspondence between slow neural oscillatory
524 phase and behaviour (using an analysis approach that does not employ shuffling-in-time),
525 consistent with the notion that distractibility is rhythmic. Future advancements in the analysis
526 approach to directly test the periodicity in cognition will further strengthen our understanding
527 of the distractibility dynamics.

528 **Neural dynamics of distractibility originate in inferior frontal/insular cortices**

529 The localisation of neural phase effects underlying distractibility dynamics beyond auditory
530 cortex regions might suggest that the proneness to distraction is supra-modal. In research on
531 visual distraction, brain regions in frontal and parietal cortices have been associated with
532 distractor interference in lesions (Chao & Knight, 1995) or transcranial magnetic stimulation
533 (Kanai et al., 2011; Wais et al., 2012) studies. The functional connectivity between the left
534 inferior frontal cortex and hippocampus is associated with the disruptive influence of task-
535 irrelevant visual distraction on working memory (Wais et al., 2010). While the current study
536 examined distractibility in the auditory modality, the neural origins found here overlap with
537 previous research on distraction in the visual modality.

538 The observed relationship between perceptual sensitivity and the inferior frontal/insular
539 theta phase suggests that fluctuations in distractibility may be related to the cognitive control

540 of working memory. The left inferior frontal cortex is assumed to be critical to the resolution
541 of competition between the maintenance of goal-relevant information and the interference from
542 external distraction (Irlbacher et al., 2014; Tops & Boksem, 2011; Wais et al., 2012). The
543 anterior insula is theorised as a gatekeeper to the brain regions responsible for goal-related
544 cognitive control (Molnar-Szakacs & Uddin, 2022), and is part of the ventral attention system
545 (Eckert et al., 2009). Specifically, the insular cortex may support the switching between
546 networks important to internally directed and externally directed cognition, respectively
547 (Uddin, 2015). The frontal theta rhythm is associated with cognitive control (Berger et al., 2019;
548 Cavanagh & Frank, 2014; Kamarajan et al., 2004) and the prioritization of relevant memory
549 representation (Riddle et al., 2020). Taken together, theta oscillations in the inferior frontal and
550 insular cortices may reflect the orchestration of the cognitive control system to maintain the
551 internal memory representation and suppress potentially distracting external inputs.

552 Against what might have been expected, the pre-distractor neural phase did not predict
553 fluctuations in the distractor-evoked neural response (S8 Fig). However, this null result might
554 rest on the distractor-evoked ERP being a rather unspecific proxy of distraction. Components
555 of the distractor-evoked ERP have been shown to reflect cognitive operations other than
556 distraction, such as reactive suppression (Feldmann-Wüstefeld & Vogel, 2019; Hickey et al.,
557 2009; Wang et al., 2019) or stimulus prediction (Volosin & Horváth, 2014). Distractibility
558 dynamics may only account for a small amount of variance in the distractor-evoked ERP.

559

560

Conclusions

561 The present study demonstrates that human proneness to distraction is not uniformly distributed
562 across time but fluctuates on a subsecond timescale in cycles of ~3 – 5 Hz. In the brain, time
563 windows of higher distractibility are coined by stronger neural responses to distractors.
564 Furthermore, slow neural phase in left inferior frontal/insular cortex regions explains
565 fluctuations in distractibility. These results unravel the temporal dynamics of distractibility and
566 thereby help explain human processing of an abundant kind of stimulus in increasingly
567 complex environments, that is, irrelevant and distracting input.

568

569

Acknowledgments

570 We thank Frauke Kraus and Malte Naujokat for their help in data collection.

571

572

573

References

574 Berger, B., Griesmayr, B., Minarik, T., Biel, A. L., Pinal, D., Sterr, A., & Sauseng, P. (2019). Dynamic
575 regulation of interregional cortical communication by slow brain oscillations during working memory.
576 *Nature Communications*, 10(1), 4242. <https://doi.org/10.1038/s41467-019-12057-0>

577 Bonnefond, M., & Jensen, O. (2012). Alpha oscillations serve to protect working memory maintenance against
578 anticipated distractors. *Current Biology*, 22(20), 1969–1974. <https://doi.org/10.1016/j.cub.2012.08.029>

579 Brainard, D. H. (1997). The Psychophysics Toolbox. *Spatial Vision*, 10(4), 433–436.
580 <https://doi.org/10.1163/156856897X00357>

581 Brookshire, G. (2022). Putative rhythms in attentional switching can be explained by aperiodic temporal
582 structure. *Nature Human Behaviour*. <https://doi.org/10.1038/s41562-022-01364-0>

583 Buschman, T. J., & Kastner, S. (2015). From Behavior to Neural Dynamics: An Integrated Theory of Attention.
584 *Neuron*, 88(1), 127–144. <https://doi.org/10.1016/j.neuron.2015.09.017>

585 Campbell, K. L., Grady, C. L., Ng, C., & Hasher, L. (2012). Age differences in the frontoparietal cognitive
586 control network: Implications for distractibility. *Neuropsychologia*, 50(9), 2212–2223.
587 <https://doi.org/10.1016/j.neuropsychologia.2012.05.025>

588 Cavanagh, J. F., & Frank, M. J. (2014). Frontal theta as a mechanism for cognitive control. *Trends in Cognitive
589 Sciences*, 18(8), 414–421. <https://doi.org/10.1016/j.tics.2014.04.012>

590 Chao, L., & Knight, R. T. (1995). Human prefrontal lesions increase distractibility to irrelevant sensory inputs.
591 *Neuroreport: An International Journal for the Rapid Communication of Research in Neuroscience*,
592 6(12), 1605–1610. <https://doi.org/10.1097/00001756-199508000-00005>

593 Cruzat, J., Torralba, M., Ruzzoli, M., Fernández, A., Deco, G., & Soto-Faraco, S. (2021). The phase of Theta
594 oscillations modulates successful memory formation at encoding. *Neuropsychologia*, 154, 107775.
595 <https://doi.org/10.1016/j.neuropsychologia.2021.107775>

596 Desimone, R., & Duncan, J. (1995). Neural mechanisms of selective visual attention. *Annual Review of
597 Neuroscience*, 18(1), 193–222.

598 Ding, N., & Simon, J. Z. (2009). Neural representations of complex temporal modulations in the human
599 auditory cortex. *Journal of Neurophysiology*, 102(5), 2731–2743.
600 <https://doi.org/10.1152/jn.00523.2009>

601 Dugué, L., & VanRullen, R. (2017). Transcranial magnetic stimulation reveals intrinsic perceptual and
602 attentional rhythms. *Frontiers in Neuroscience*, 11. <https://doi.org/10.3389/fnins.2017.00154>

603 Dürschmid, S., Reichert, C., Hinrichs, H., Heinze, H.-J., Kirsch, H. E., Knight, R. T., & Deouell, L. Y. (n.d.).
604 Direct evidence for prediction signals in frontal cortex independent of prediction error. *Cerebral
605 Cortex*, 1–9. <https://doi.org/10.1093/cercor/bhy331>

606 Eckert, M. A., Menon, V., Walczak, A., Ahlstrom, J., Denslow, S., Horwitz, A., & Dubno, J. R. (2009). At the
607 heart of the ventral attention system: The right anterior insula. *Human Brain Mapping*, 30(8), 2530–
608 2541. <https://doi.org/10.1002/hbm.20688>

609 Feldmann-Wüstefeld, T., & Vogel, E. K. (2019). Neural Evidence for the Contribution of Active Suppression
610 During Working Memory Filtering. *Cerebral Cortex*, 29(2), 529–543.
611 <https://doi.org/10.1093/cercor/bhx336>

612 Fiebelkorn, I. C. (2022). Detecting attention-related rhythms: When is behavior not enough? (Commentary on
613 van der Werf et al. 2021). *European Journal of Neuroscience*, 55(11–12), 3117–3120.
614 <https://doi.org/10.1111/ejn.15322>

615 Fiebelkorn, I. C., & Kastner, S. (2019). A Rhythmic Theory of Attention. *Trends in Cognitive Sciences*, 23(2),
616 87–101. <https://doi.org/10.1016/j.tics.2018.11.009>

617 Fiebelkorn, I. C., Saalmann, Y. B., & Kastner, S. (2013). Rhythmic Sampling within and between objects
618 despite sustained attention at a cued location. *Current Biology*, 23(24), 2553–2558.
619 <https://doi.org/10.1016/j.cub.2013.10.063>

620 Forster, S., & Lavie, N. (2014). Distracted by your mind? Individual differences in distractibility predict mind
621 wandering. *Journal of Experimental Psychology: Learning, Memory, and Cognition*, 40(1), 251–260.
622 <https://doi.org/10.1037/a0034108>

623 Geng, J. J. (2014). Attentional mechanisms of distractor suppression. *Current Directions in Psychological
624 Science*, 23(2), 147–153. <https://doi.org/10.1177/0963721414525780>

625 Geng, J. J., & DiQuattro, N. E. (2010). Attentional capture by a perceptually salient non-target facilitates target
626 processing through inhibition and rapid rejection. *Journal of Vision*, 10(6), 1–12.
627 <https://doi.org/10.1167/10.6.5>

628 Grabenhorst, M., Maloney, L. T., Poeppel, D., & Michalareas, G. (2021). Two sources of uncertainty
629 independently modulate temporal expectancy. *Proceedings of the National Academy of Sciences*,
630 118(16), e2019342118. <https://doi.org/10.1073/pnas.2019342118>

631 Helfrich, R. F., Fiebelkorn, I. C., Szczerpanski, S. M., Lin, J. J., Parvizi, J., Knight, R. T., & Kastner, S. (2018).
632 Neural mechanisms of sustained attention are rhythmic. *Neuron*, 99(4), 854-865.e5.
633 <https://doi.org/10.1016/j.neuron.2018.07.032>

634 Herbst, S. K., Stefanics, G., & Obleser, J. (2022). Endogenous modulation of delta phase by expectation—A
635 replication of Stefanics et al., 2010. *Cortex*, 149, 226–245. <https://doi.org/10.1016/j.cortex.2022.02.001>

636 Hickey, C., Di Lollo, V., & McDonald, J. J. (2009). Electrophysiological Indices of Target and Distractor
637 Processing in Visual Search. *Journal of Cognitive Neuroscience*, 21(4), 760–775.
638 <https://doi.org/10.1162/jocn.2009.21039>

639 Ho, H. T., Leung, J., Burr, D. C., Alais, D., & Morrone, M. C. (2017). Auditory sensitivity and decision criteria
640 oscillate at different frequencies separately for the two ears. *Current Biology*, 27(23), 3643-3649.e3.
641 <https://doi.org/10.1016/j.cub.2017.10.017>

642 Huang, Y., Chen, L., & Luo, H. (2015). Behavioral oscillation in priming: Competing perceptual predictions
643 conveyed in alternating theta-band rhythms. *Journal of Neuroscience*, 35(6), 2830–2837.
644 <https://doi.org/10.1523/JNEUROSCI.4294-14.2015>

645 Irlbacher, K., Kraft, A., Kehrer, S., & Brandt, S. A. (2014). Mechanisms and neuronal networks involved in
646 reactive and proactive cognitive control of interference in working memory. *Neuroscience &*
647 *Biobehavioral Reviews*, 46, 58–70. <https://doi.org/10.1016/j.neubiorev.2014.06.014>

648 Kamarajan, C., Porjesz, B., Jones, K. A., Choi, K., Chorlian, D. B., Padmanabhapillai, A., Rangaswamy, M.,
649 Stimus, A. T., & Begleiter, H. (2004). The role of brain oscillations as functional correlates of
650 cognitive systems: A study of frontal inhibitory control in alcoholism. *International Journal of*
651 *Psychophysiology*, 51(2), 155–180. <https://doi.org/10.1016/j.ijpsycho.2003.09.004>

652 Kanai, R., Dong, M. Y., Bahrami, B., & Rees, G. (2011). Distractibility in daily life Is reflected in the structure
653 and function of human parietal cortex. *Journal of Neuroscience*, 31(18), 6620–6626.
654 <https://doi.org/10.1523/JNEUROSCI.5864-10.2011>

655 Kannass, K. N., Oakes, L. M., & Shaddy, D. J. (2006). A longitudinal investigation of the development of
656 attention and distractibility. *Journal of Cognition and Development*, 7(3), 381–409.
657 https://doi.org/10.1207/s15327647jcd0703_8

658 Koerner, T. K., & Zhang, Y. (2015). Effects of background noise on inter-trial phase coherence and auditory
659 N1–P2 responses to speech stimuli. *Hearing Research*, 328, 113–119.
660 <https://doi.org/10.1016/j.heares.2015.08.002>

661 Kubetschek, C., & Kayser, C. (2021). Delta/Theta band EEG activity shapes the rhythmic perceptual sampling
662 of auditory scenes. *Scientific Reports*, 11(2370), 2370. <https://doi.org/10.1101/2020.07.21.213694>

663 Lakatos, P., Shah, A. S., Knuth, K. H., Ulbert, I., Karmos, G., & Schroeder, C. E. (2005). An Oscillatory
664 Hierarchy Controlling Neuronal Excitability and Stimulus Processing in the Auditory Cortex. *Journal
665 of Neurophysiology*, 94(3), 1904–1911. <https://doi.org/10.1152/jn.00263.2005>

666 Landau, A. N., & Fries, P. (2012). Attention samples stimuli rhythmically. *Current Biology*, 22(11), 1000–1004.
667 <https://doi.org/10.1016/j.cub.2012.03.054>

668 Lui, T. K.-Y., & Wöstmann, M. (2022). Effects of temporally regular versus irregular distractors on goal-
669 directed cognition and behavior. *Scientific Reports*, 12, 10020. [https://doi.org/10.1038/s41598-022-13211-3](https://doi.org/10.1038/s41598-022-
670 13211-3)

671 Macmillan, N. A., & Kaplan, H. L. (1985). Detection theory analysis of group data: Estimating sensitivity from
672 average hit and false-alarm rates. *Psychological Bulletin*, 98(1), 185–199. [https://doi.org/10.1037/0033-2909.98.1.185](https://doi.org/10.1037/0033-
673 2909.98.1.185)

674 Maris, E., & Oostenveld, R. (2007). Nonparametric statistical testing of EEG- and MEG-data. *Journal of
675 Neuroscience Methods*, 164(1), 177–190. <https://doi.org/10.1016/j.jneumeth.2007.03.024>

676 Mayhew, S. D., Dirckx, S. G., Niazy, R. K., Iannetti, G. D., & Wise, R. G. (2010). EEG signatures of auditory
677 activity correlate with simultaneously recorded fMRI responses in humans. *NeuroImage*, 49(1), 849–
678 864. <https://doi.org/10.1016/j.neuroimage.2009.06.080>

679 Molnar-Szakacs, I., & Uddin, L. Q. (2022). Anterior insula as a gatekeeper of executive control. *Neuroscience
680 & Biobehavioral Reviews*, 139, 104736. <https://doi.org/10.1016/j.neubiorev.2022.104736>

681 Noonan, M. P., Adamian, N., Pike, A., Printzlau, F., Crittenden, B. M., & Stokes, M. G. (2016). Distinct
682 mechanisms for distractor suppression and target facilitation. *The Journal of Neuroscience*, 36(6),
683 1797–1807. <https://doi.org/10.1523/JNEUROSCI.2133-15.2016>

684 Oldfield, R. C. (1971). The assessment and analysis of handedness: The Edinburgh inventory.
685 *Neuropsychologia*, 9(1), 97–113. [https://doi.org/10.1016/0028-3932\(71\)90067-4](https://doi.org/10.1016/0028-3932(71)90067-4)

686 Oostenveld, R., Fries, P., Maris, E., & Schoffelen, J.-M. (2011). FieldTrip: Open source software for advanced
687 analysis of MEG, EEG, and invasive electrophysiological data. *Computational Intelligence and*
688 *Neuroscience*, 2011, 156869. <https://doi.org/10.1155/2011/156869>

689 Oya, H., Gander, P. E., Petkov, C. I., Adolphs, R., Nourski, K. V., Kawasaki, H., Howard, M. A., & Griffiths, T.
690 D. (2018). Neural phase locking predicts BOLD response in human auditory cortex. *NeuroImage*, 169,
691 286–301. <https://doi.org/10.1016/j.neuroimage.2017.12.051>

692 Picton, T. W., Hillyard, S. A., Galambos, R., & Schiff, M. (1971). Human auditory attention: A central or
693 peripheral process? *Science*, 173(3994), 351–353.

694 Posner, M. I., Snyder, C. R., & Davidson, B. J. (1980). Attention and the detection of signals. *Journal of*
695 *Experimental Psychology: General*, 109(2), 160–174. <https://doi.org/10.1037/0096-3445.109.2.160>

696 Prins, N., & Kingdom, F. A. A. (2018). Applying the model-comparison approach to test specific research
697 hypotheses in psychophysical research using the palamedes toolbox. *Frontiers in Psychology*, 9, 1250.
698 <https://doi.org/10.3389/fpsyg.2018.01250>

699 Riddle, J., Scimeca, J. M., Cellier, D., Dhanani, S., & D'Esposito, M. (2020). Causal evidence for a role of theta
700 and alpha oscillations in the control of working memory. *Current Biology*, 30(9), 1748-1754.e4.
701 <https://doi.org/10.1016/j.cub.2020.02.065>

702 Rutishauser, U., Ross, I. B., Mamelak, A. N., & Schuman, E. M. (2010). Human memory strength is predicted
703 by theta-frequency phase-locking of single neurons. *Nature*, 464(7290), 903–907.
704 <https://doi.org/10.1038/nature08860>

705 Schmid, R. R., Pomper, U., & Ansorge, U. (2022). Cyclic reactivation of distinct feature dimensions in human
706 visual working memory. *Acta Psychologica*, 226, 103561.
707 <https://doi.org/10.1016/j.actpsy.2022.103561>

708 Schneider, D., Göddertz, A., Haase, H., Hickey, C., & Wascher, E. (2018). Hemispheric asymmetries in EEG
709 alpha oscillations indicate active inhibition during attentional orienting within working memory.
710 *Behavioural Brain Research*, 359, 38–46. <https://doi.org/10.1016/j.bbr.2018.10.020>

711 Schneider, D., Herbst, S. K., Klatt, L., & Wöstmann, M. (2021). Target enhancement or distractor suppression?
712 Functionally distinct alpha oscillations form the basis of attention. *European Journal of Neuroscience*,
713 ejn.15309. <https://doi.org/10.1111/ejn.15309>

714 Shamma, S. A., Elhilali, M., & Micheyl, C. (2011). Temporal coherence and attention in auditory scene
715 analysis. *Trends in Neurosciences*, 34(3), 114–123. <https://doi.org/10.1016/j.tins.2010.11.002>

716 Siegel, M., Warden, M. R., & Miller, E. K. (2009). Phase-dependent neuronal coding of objects in short-term
717 memory. *Proceedings of the National Academy of Sciences*, 106(50), 21341–21346.
718 <https://doi.org/10.1073/pnas.0908193106>

719 Stefanics, G., Hangya, B., Hernadi, I., Winkler, I., Lakatos, P., & Ulbert, I. (2010). Phase entrainment of human
720 delta oscillations can mediate the effects of expectation on reaction speed. *Journal of Neuroscience*,
721 30(41), 13578–13585. <https://doi.org/10.1523/JNEUROSCI.0703-10.2010>

722 ter Wal, M., Linde-Domingo, J., Lifanov, J., Roux, F., Kolibius, L. D., Gollwitzer, S., Lang, J., Hamer, H.,
723 Rollings, D., Sawlani, V., Chelvarajah, R., Staresina, B., Hanslmayr, S., & Wimber, M. (2021). Theta
724 rhythmicity governs human behavior and hippocampal signals during memory-dependent tasks. *Nature
725 Communications*, 12(1), 7048. <https://doi.org/10.1038/s41467-021-27323-3>

726 Tops, M., & Boksem, M. A. S. (2011). A potential role of the inferior frontal gyrus and anterior insula in
727 cognitive control, brain rhythms, and event-related potentials. *Frontiers in Psychology*, 2.
728 <https://doi.org/10.3389/fpsyg.2011.00330>

729 Uddin, L. Q. (2015). Salience processing and insular cortical function and dysfunction. *Nature Reviews
730 Neuroscience*, 16(1), 55–61. <https://doi.org/10.1038/nrn3857>

731 van Moorselaar, D., Lampers, E., Cordesius, E., & Slagter, H. A. (2020). Neural mechanisms underlying
732 expectation-dependent inhibition of distracting information. *ELife*, 9, e61048.
733 <https://doi.org/10.7554/eLife.61048>

734 Van Veen, B. D., Van Drongelen, W., Yuchtman, M., & Suzuki, A. (1997). Localization of brain electrical
735 activity via linearly constrained minimum variance spatial filtering. *IEEE Transactions on Biomedical
736 Engineering*, 44(9), 867–880. <https://doi.org/10.1109/10.623056>

737 VanRullen, R. (2016). Perceptual Cycles. *Trends in Cognitive Sciences*, 20(10), 723–735.
738 <https://doi.org/10.1016/j.tics.2016.07.006>

739 Volosin, M., & Horváth, J. (2014). Knowledge of sequence structure prevents auditory distraction: An ERP
740 study. *International Journal of Psychophysiology*, 92(3), 93–98.
741 <https://doi.org/10.1016/j.ijpsycho.2014.03.003>

742 Wais, P. E., Kim, O. Y., & Gazzaley, A. (2012). Distractibility during episodic retrieval is exacerbated by
743 perturbation of left ventrolateral prefrontal cortex. *Cerebral Cortex*, 22(3), 717–724.
744 <https://doi.org/10.1093/cercor/bhr160>

745 Wais, P. E., Rubens, M. T., Boccanfuso, J., & Gazzaley, A. (2010). Neural mechanisms underlying the impact
746 of visual distraction on retrieval of long-term memory. *Journal of Neuroscience*, 30(25), 8541–8550.
747 <https://doi.org/10.1523/JNEUROSCI.1478-10.2010>

748 Wang, B., van Driel, J., Ort, E., & Theeuwes, J. (2019). Anticipatory Distractor Suppression Elicited by
749 Statistical Regularities in Visual Search. *Journal of Cognitive Neuroscience*, 31(10), 1535–1548.
750 https://doi.org/10.1162/jocn_a_01433

751 Weisz, N., Kraft, N. G., & Demarchi, G. (2020). Auditory cortical alpha/beta desynchronization prioritizes the
752 representation of memory items during a retention period. *eLife*, 9, e55508.
753 <https://doi.org/10.7554/eLife.55508>

754 Wöstmann, M. (2022). Does attention follow a rhythm? *Nature Human Behaviour*.
755 <https://doi.org/10.1038/s41562-022-01365-z>

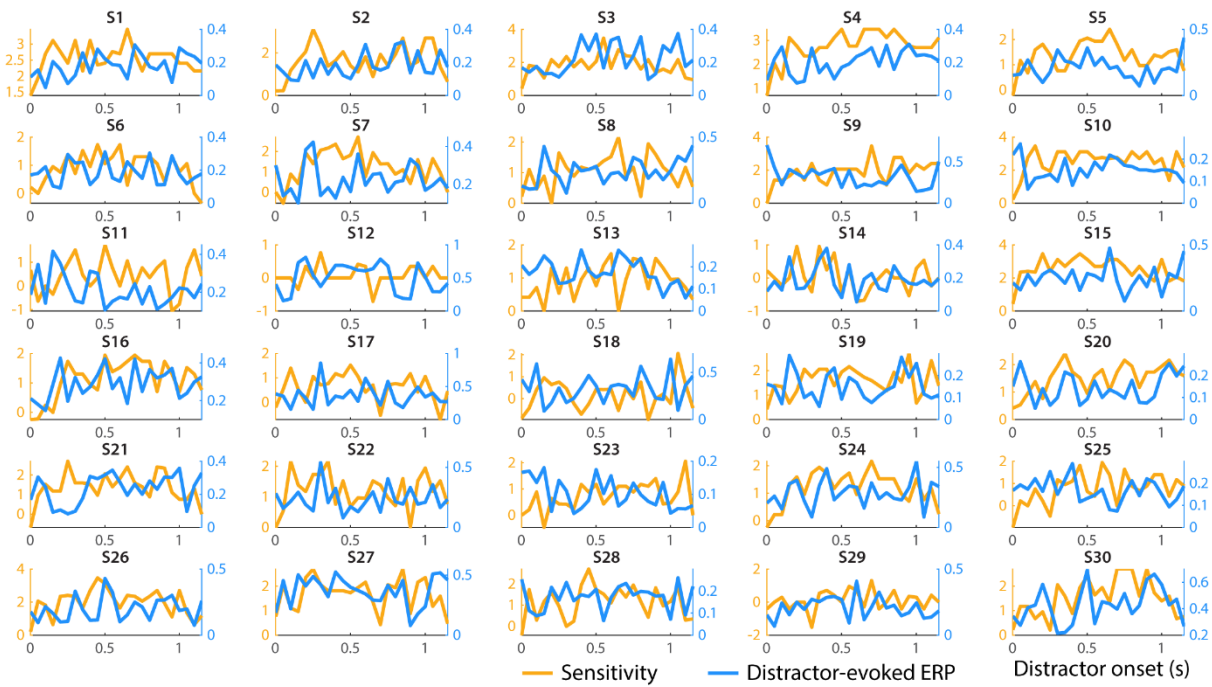
756 Wöstmann, M., Alavash, M., & Obleser, J. (2019). Alpha oscillations in the human brain implement distractor
757 suppression independent of target selection. *The Journal of Neuroscience*, 39(49), 9797–9805.
758 <https://doi.org/10.1523/JNEUROSCI.1954-19.2019>

759 Wöstmann, M., Lui, T. K.-Y., Friese, K.-H., Kreitewolf, J., Naujokat, M., & Obleser, J. (2020). The
760 vulnerability of working memory to distraction is rhythmic. *Neuropsychologia*, 146, 107505.
761 <https://doi.org/10.1016/j.neuropsychologia.2020.107505>

762 Wöstmann, M., Störmer, V. S., Obleser, J., Addleman, D. A., Andersen, S. K., Gaspelin, N., Geng, J. J., Luck,
763 S. J., Noonan, M. P., Slagter, H. A., & Theeuwes, J. (2022). Ten simple rules to study distractor
764 suppression. *Progress in Neurobiology*, 213, 102269. <https://doi.org/10.1016/j.pneurobio.2022.102269>

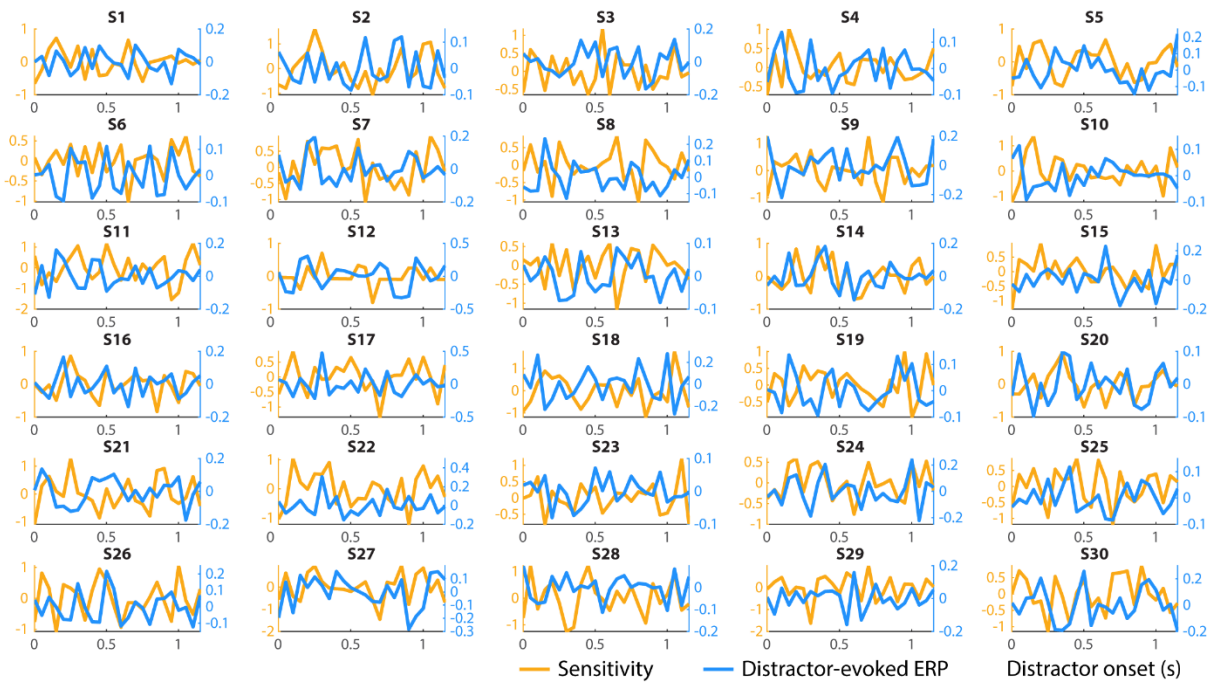
765 Zoefel, B., Davis, M. H., Valente, G., & Riecke, L. (2019). How to test for phasic modulation of neural and
766 behavioural responses. *NeuroImage*, 202, 116175. <https://doi.org/10.1016/j.neuroimage.2019.116175>

767



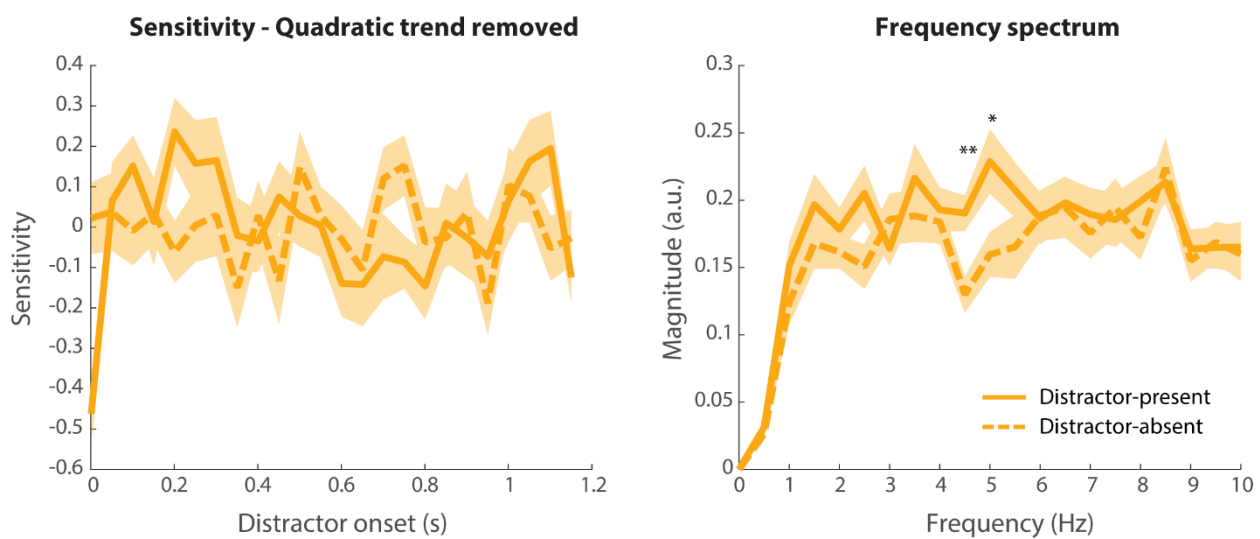
768

769 **Fig. S1. Individual time courses of raw sensitivity (yellow) and distractor-evoked ERP (25-Hz amplitude of distractor-
770 evoked ERP; blue).**



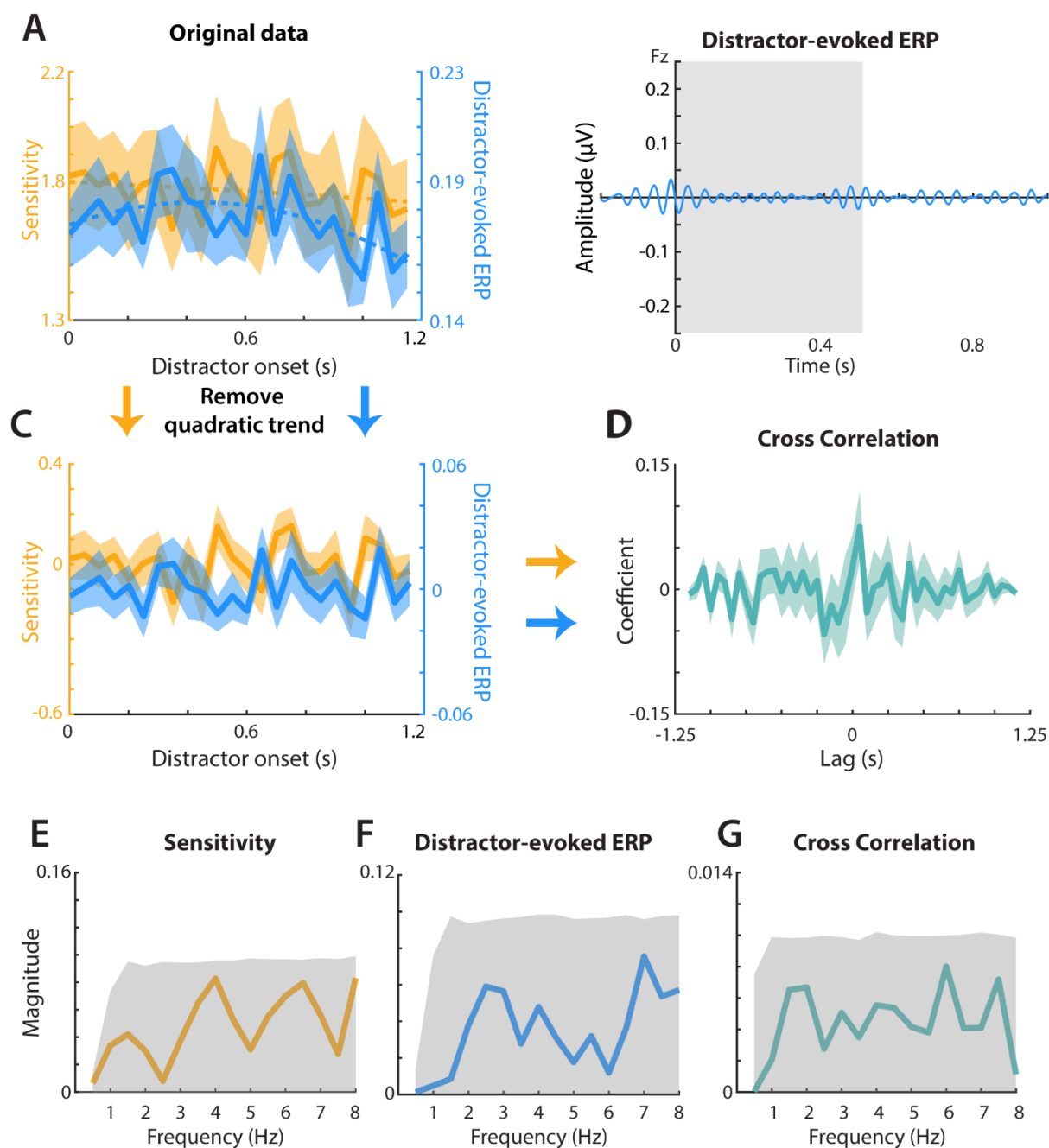
771

772 **Fig. S2. Detrended (quadratic trend removed) sensitivity (yellow) and distractor-evoked ERP (blue) individual time**
773 **courses.**

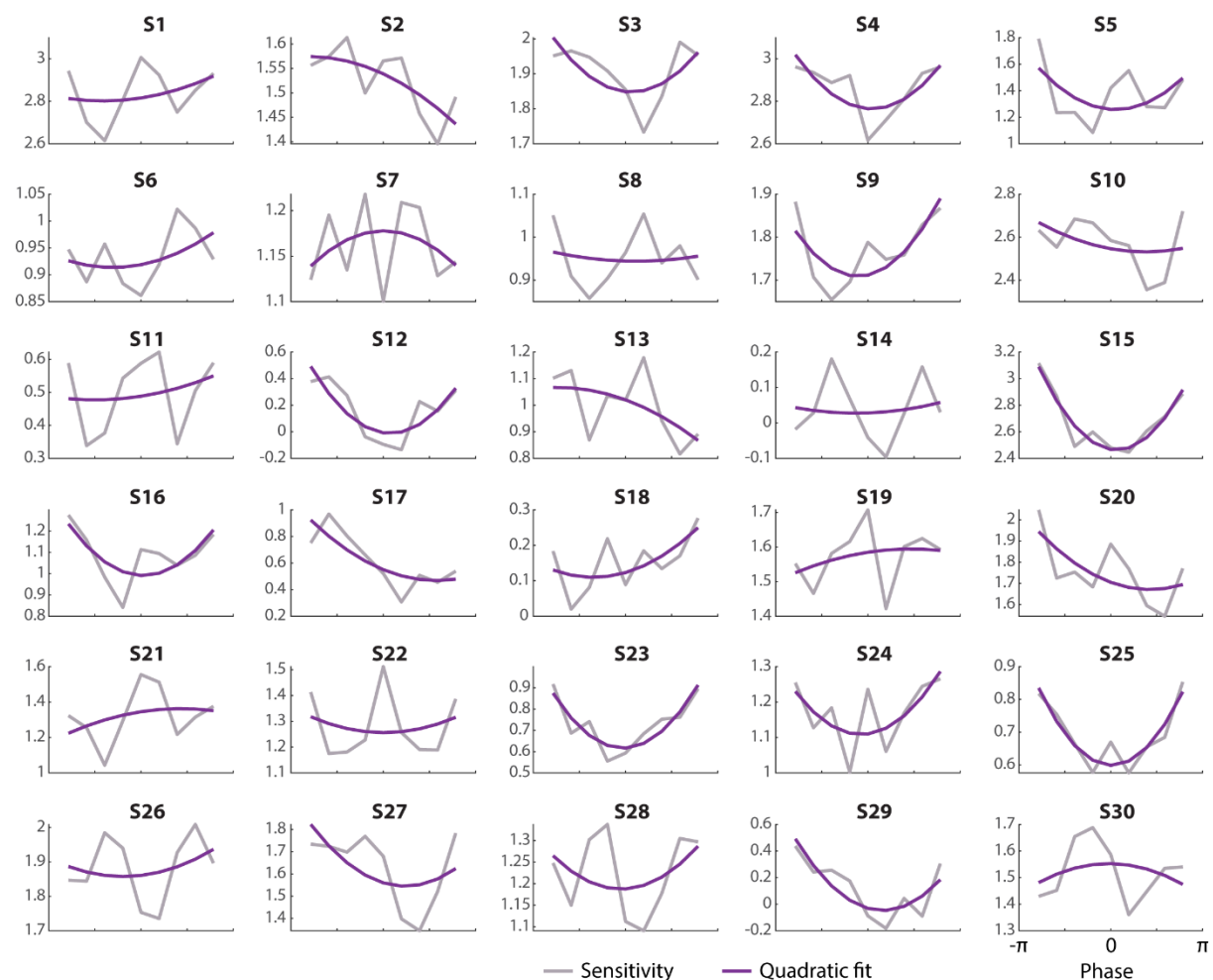


774

775 **Fig. S3. Comparison of the spectral magnitude between distractor-present and distractor-absent conditions.** Left panel
776 shows the sensitivity time courses for distractor-present (solid) and distractor-absent (dashed) conditions. Right panel shows
777 the averaged frequency spectra, derived from FFT on single-subject time courses. Shaded areas show ± 1 SEM across individual
778 participants. Asterisks show statistical significance when comparing the spectral magnitude of distractor-present versus -absent
779 conditions (using uncorrected dependent-samples t-tests). * $p < .05$ ** $p < .01$

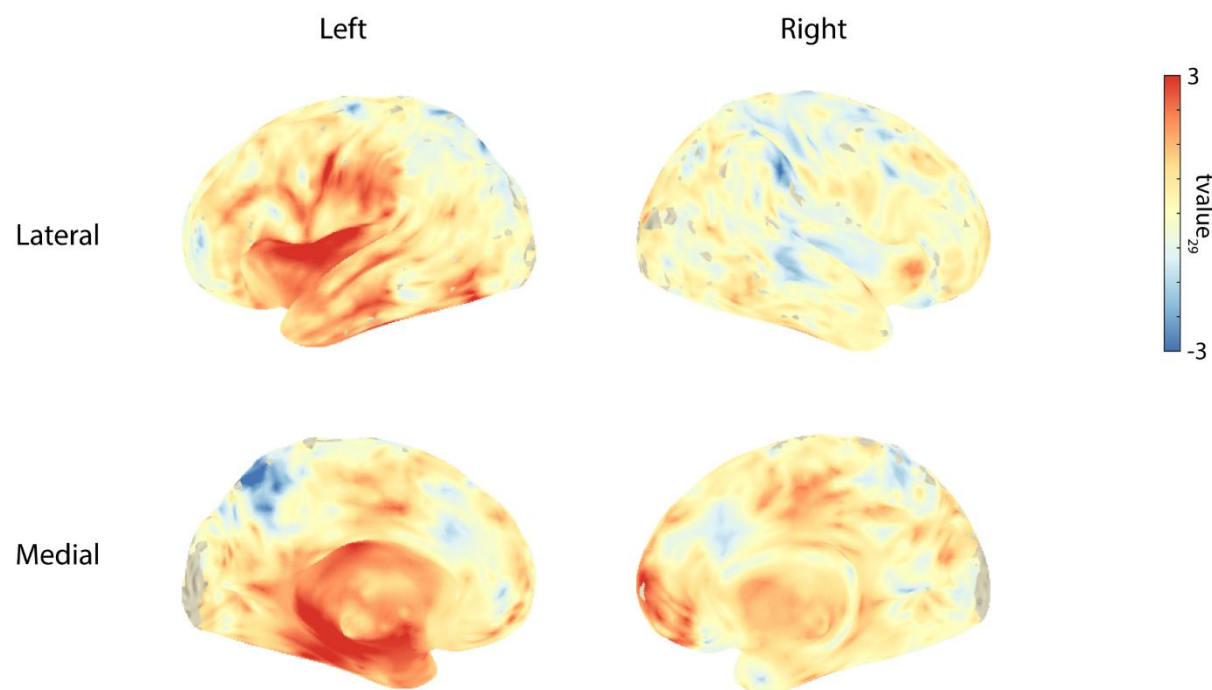


781 **Fig. S4.** The same analysis pipeline as shown in Fig 2 applied to the distractor-absent condition.



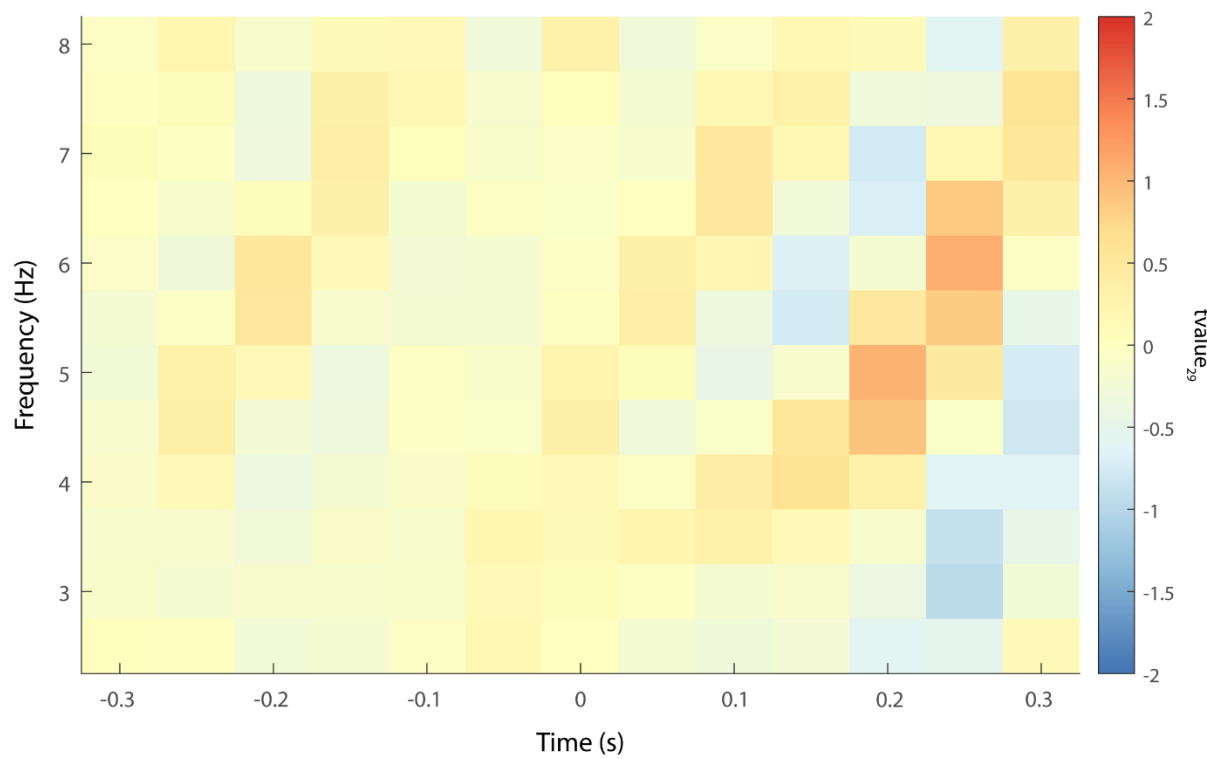
782

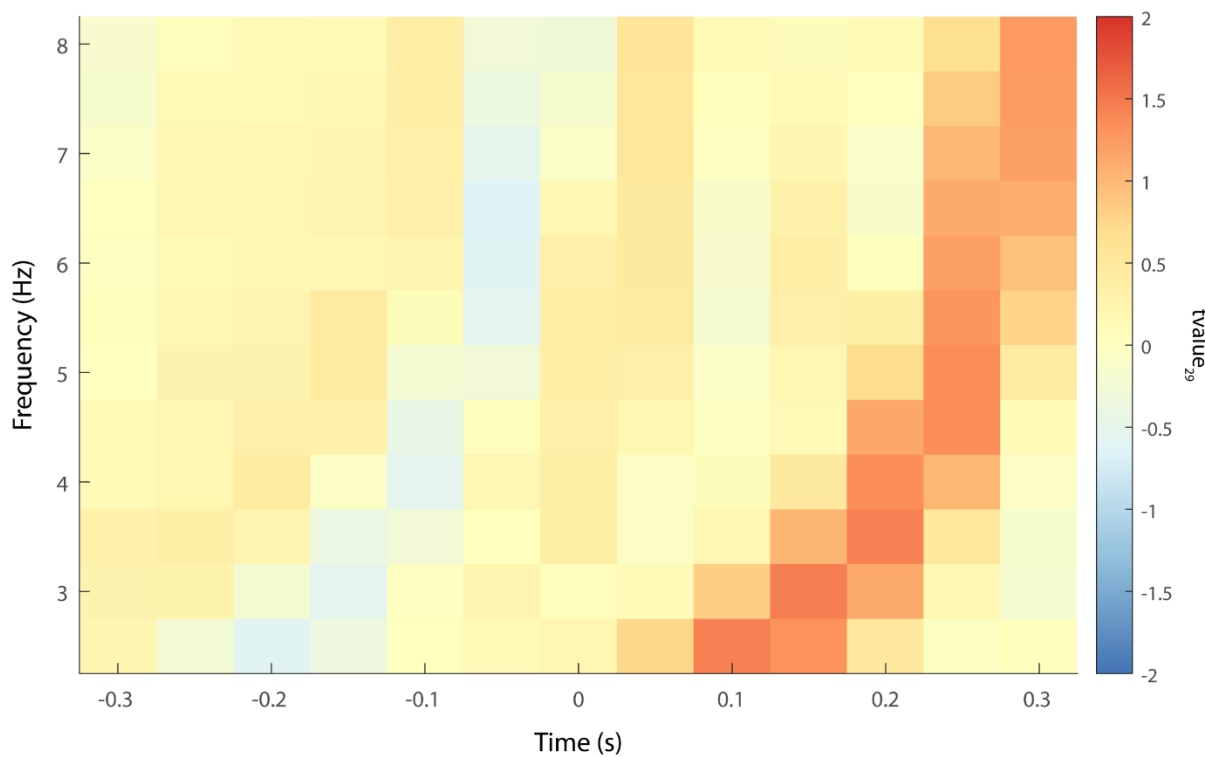
783 **Fig. S5. Individual sensitivity (grey line) and quadratic fit (purple line) across phase bins of the significant positive**
784 **cluster at 3 Hz.**



785

786 **Fig. S6. Brain surface plots of the cluster peak effect.** Brain surface plots of the cluster peak effect (3 Hz; -0.2 s) from left
787 lateral (top left), right lateral (top right), left medial (bottom left), and right medial (bottom right) views show t-values for the
788 comparison of the quadratic fit of the sensitivity sorted by phase bins against zero. The t-values were interpolated and projected
789 onto MNI coordinates for visualization purposes.





796

Time (s)

797 **Fig. S8. Cluster-based permutation test on distractor-evoked ERP amplitude.** Results of the cluster-based permutation
798 test, across time windows and frequencies, on the quadratic relationship between neural phase and distractor-evoked ERP
799 amplitude at 25 Hz. Figure shows t-values ($df = 29$) averaged across all the voxels belonging to the significant positive cluster
800 testing the quadratic relationship between neural phase and behavioural sensitivity shown in Figure 3. As expected, and not of
801 main interest in the current study, a significant cluster in the post-stimulus time window (i.e., >0 s) was found. More importantly,
802 no significant cluster was found in the pre-distractor time window (i.e., <0 s).